



Connectivity dependence of gelation and elasticity in AB-type polymerization: An experimental comparison of dynamic process and stoichiometrically imbalanced mixing

Journal:	<i>Soft Matter</i>
Manuscript ID	SM-ART-04-2019-000696.R1
Article Type:	Paper
Date Submitted by the Author:	09-May-2019
Complete List of Authors:	Yoshikawa, Yuuki; The University of Tokyo, Graduate School of Engineering, Department of Materials Engineering Sakumichi, Naoyuki; The University of Tokyo, Graduate School of Engineering, Department of Materials Engineering Chung, Ung-il; The University of Tokyo, Sakai, Takamasa; The University of Tokyo, Graduate School of Engineering, Department of Materials Engineering

Submitted to Soft Matter

Connectivity dependence of gelation and elasticity in AB-type polymerization: An experimental comparison of dynamic process and stoichiometrically imbalanced mixing

Yuki Yoshikawa^a, Naoyuki Sakumichi^a, Ung-il Chung^a, Takamasa Sakai^{a*}

^aDepartment of Bioengineering, Graduate School of Engineering, The University of Tokyo
7-3-1 Hongo, Bunkyo-ku, Tokyo, Japan

*Corresponding to be addressed

sakai@tetrapod.t.u-tokyo.ac.jp

Abstract

To control various physical properties of polymer gels, it is important to control the connection probability between functional groups of network structure (connectivity). In this study, we compare two methodologies tuning the connectivity in AB-type polymerization: one is stopping the reaction intentionally at a certain conversion, and the other is mixing two prepolymers in a stoichiometrically imbalanced ratio. By experimentally examining relationships between elastic modulus and connectivity, we find that the relationships are almost the same for these two methodologies. However, critical connectivity for gelation is different. These results are well reproduced by a kind of the phantom network model whose structural parameters are estimated by using a mean-field approximation.

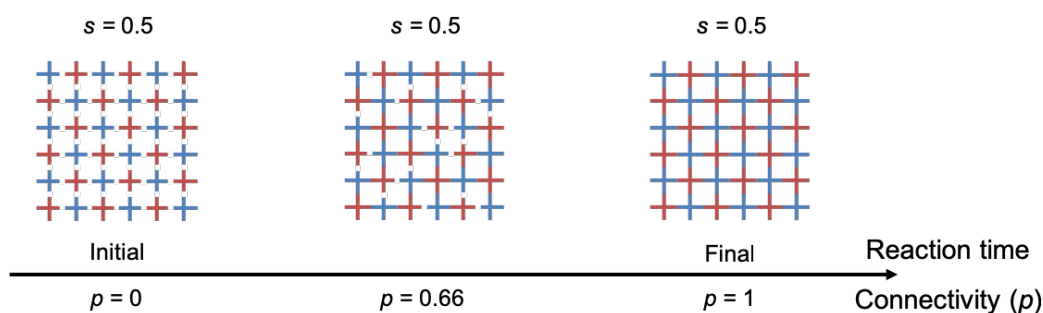
Introduction

AB-type polymerization is often used for a formation process of various gels including injectable gels, which draw much attention as a new class of biomaterials.¹⁻³ In the AB-type polymerization, gels can be further functionalized through the reaction to the residual functional groups, and control over physical properties is possible by tuning the ratio of A to B species. Such modifications intentionally or unintentionally change the connectivity (p), which is defined as the fraction of reacted A and B groups in this paper. Therefore, it is important to understand the effect of connectivity on physical properties for practical applications.

We compare two methodologies tuning the connectivity of AB-type polymerization: dynamic process (DP) and stoichiometrically imbalanced mixing (IM). These methods are mainly used for the study of gelation. In the DP, two prepolymers are mixed in a stoichiometric ratio and the reaction is intentionally stopped at a certain conversion (Fig. 1 (a)).⁴⁻⁷ In many cases, the DP is achieved by quenching the reaction during the dynamic process of gelation. In the IM, two prepolymers are mixed in a stoichiometrically imbalanced ratio, and as a result, the connectivity after completion of the reaction is tuned (Fig. 1 (b)).⁸⁻¹⁶ To parameterize this ratio, we define the mixing fraction s as the fraction of functional groups that is type A before starting reaction, i.e., $[A] : [B] = s : 1-s$ ($0 \leq s \leq 1$). In order to treat $[A]$ and $[B]$ equally, we use the mixing fraction $s = [A]/([A]+[B])$ in this paper instead of the mixing ratio $[A]/[B]$. In addition to the study of gelation, to study the IM is important because this method to synthesize

highly branched polymers¹⁷ is widely applied for commercial products such as 2K coatings and adhesives.

(a) The dynamic process (DP)



(b) The stoichiometrically imbalanced mixing (IM)

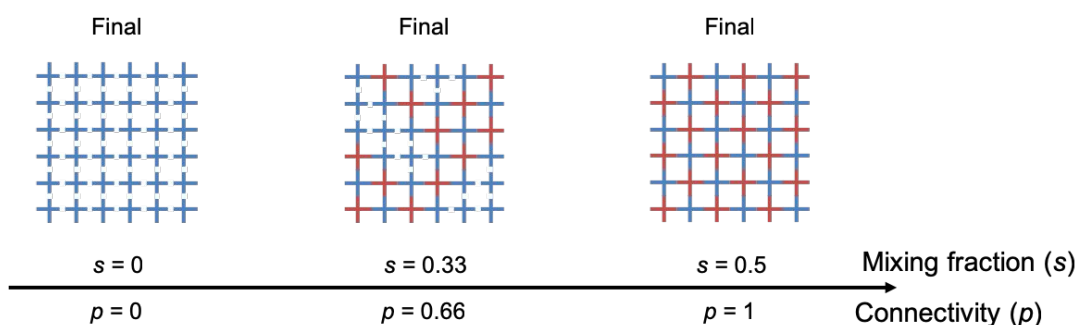


Fig. 1 (a) Schematic illustration of the dynamic process (DP), where two prepolymers are mixed in a stoichiometric ratio ($s = 0.5$) ([red tetra-functional prepolymers] : [blue tetra-functional prepolymers] = $s : 1-s$ ($0 \leq s \leq 1$)) and the reaction is intentionally stopped at a certain conversion. (b) Schematic illustration of the stoichiometrically imbalanced mixing (IM), where two prepolymers are mixed in a stoichiometrically imbalanced ratio ($s \neq 0.5$) and the connectivity after completion of the reaction is tuned. The connectivity (ρ) is determined from s in accordance with Eq. (1) assuming completion of the reaction of the minor group, i.e., $p_A = 1$ and $p_B = s/(1-s)$. Note that in this experiment, p_A is the terminal functionalization fraction of the minor group.

Recently, we investigated the DP: the effect of connectivity on physical properties including elastic modulus,^{18,19} fracture energy,²⁰ and ultimate elongation ratio.²¹ As for the elastic modulus (G), in high connectivity ($p > 0.75$), we found that the connectivity dependence of the elastic modulus were well reproduced by a kind of the phantom network model²² whose structural parameters were estimated by using a mean-field approximation (MF)^{23–25} (the details are described in the theoretical and discussion section).²⁶ Therefore, MF may roughly capture the mechanical properties of gelation.

In this paper, we investigated the connectivity dependence of the elastic modulus both in the DP and IM with tuned prepolymer concentration by using Tetra-PEG gel,²⁷ which is formed by AB-type polymerization of tetra-functional prepolymers, as a model system. The critical connectivity for gelation (p_c) were investigated as well. These data were compared to the prediction by MF. The phantom network model using MF predicts that the connectivity dependence of the elastic modulus is different between DP and IM. This difference originates from the difference in the correlation between the connectivity defects based on MF. Our results strongly suggest the applicability of MF to AB-type polymerizations.

Theoretical section

We consider Tetra-PEG gels formed by a stepwise AB-type copolymerization of two non-equimolar tetra-functional prepolymers (A_4 and B_4). We define s as the fraction of functional groups that is type A before starting reaction, i.e., $[A_4] : [B_4] = s : 1-s$ ($0 \leq s \leq 1$). Under the given s , the properties of the system are determined by the connectivity (p), which is defined as the fraction of reacted A and B groups, i.e., the weighted averaged connection probability between the tetra-functional prepolymers:

$$p = s p_A + (1 - s) p_B, \# (1)$$

where p_A and p_B are the fractions of reacted A and B groups, respectively. We note that p is the common variable in the dynamic process (DP) and the stoichiometrically imbalanced mixing (IM), which enables us to compare these methods.

In this study, we compare the elastic modulus in the DP and the IM. In the DP, we tune the connectivity by stopping the reaction intentionally at a certain conversion in the stoichiometric condition of A_4 and B_4 species (i.e., $s=1/2$). We note that a stoichiometric system satisfies $p_A = p_B = p$, and thus is reduced to a stepwise homopolymerization (AA-type). In the IM, we tune the connectivity by mixing two kinds of prepolymers at a stoichiometrically imbalanced ratio (i.e., $s \neq 1/2$) and complete the reaction of the minor group. For simplicity, we consider $0 \leq s \leq 1/2$ (i.e., $[A_4] < [B_4]$) and thus $p_A = 1$ and $p_B = s/(1-s)$, so that from Eq. (1), the averaged connection probability in the IM is $p = 2s$. Figure 2 shows the relationship between connectivity (p) and mixing fraction (s) in the DP and the IM.

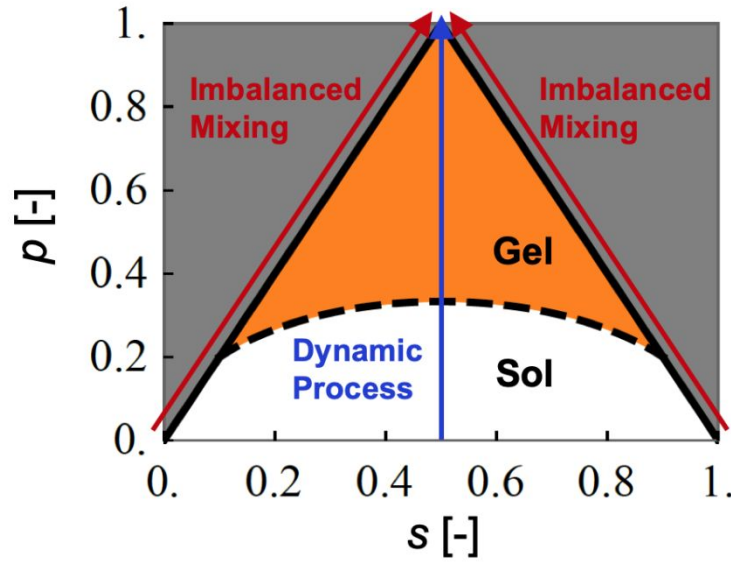


Fig. 2 Relationship between connectivity (p) and mixing fraction (s) in dynamic process (DP) and stoichiometrically imbalanced mixing (IM). Here, we assume the complete reaction of a minor group in the IM ($p_A = 1$ or $p_B = 1$).

The phantom network model²² theoretically predicts the elastic modulus (G) of elastomers (e.g., rubbers and polymer gels) as

$$G = \xi n k T, \#(2)$$

where n , k , and T are the number density of tetra-functional prepolymers, Boltzmann constant, and absolute temperature, respectively. Here,

$$\xi \equiv \nu - \mu, \#(3)$$

is the difference between the number per prepolymer of the elastically effective chains (ν) and the crosslinks (μ). The structural parameters ξ , ν , and μ are all dimensionless and satisfy the following inequations for a tetra-functional prepolymer: $0 \leq \mu \leq 1$, $0 \leq \nu \leq 2$, and $0 \leq \xi \leq 1$. In previous literature, *the number densities* of the structural

parameters, e.g., $\xi_{\text{density}} = n\xi$, are often used. In this paper, however, we use *the number* of the structural parameter (ξ) in order to focus on the contribution of network structure to the mechanical properties. Although ξ cannot be directly observed experimentally, ξ can be theoretically estimated by a mean-field approximation (MF).^{23–25} In this paper, we adopt the recursive method of Miller and Macosko^{23,24} to calculate the mean-field value (ξ^{MF}), which depends only on connectivity (p). (See Fig. 4 below.)

Our previous experiment²⁶ using the Tetra-PEG gel in the DP has shown that the similar (but different) relationship from the phantom network model as

$$G = g\xi^{\text{MF}}, \#(4)$$

in high p , and this tendency is more pronounced at higher prepolymer concentrations. Here, g is a function depending on the prepolymer concentration (C) and temperature. We note that Eqs. (2) and (4) are different; that is, g is not proportional to n . In the following, we calculate ξ^{MF} by using the recursive method^{23,24} for not only the DP but also the IM.

First, we calculate the probabilities that one arm of A_4 or B_4 does not connect to the infinite-sized network ($P(F_A^{\text{out}})$ or $P(F_B^{\text{out}})$, respectively). As shown in Fig. 3, when we regard the network structure as a tree structure, $P(F_A^{\text{out}})$ is the sum of the possibilities of (i) the event that one arm of A_4 connects to B_4 , and all remaining three arms of the connected B_4 do not connect to the infinite-sized network and (ii) the event that one arm of A_4 does not connect to B_4 :

$$P(F_A^{\text{out}}) = p_A P(F_B^{\text{out}})^3 + 1 - p_A. \#(5)$$

In the same way, we have

$$P(F_{\mathbf{B}}^{\text{out}}) = p_{\mathbf{B}}P(F_{\mathbf{A}}^{\text{out}})^3 + 1 - p_{\mathbf{B}}. \#(6)$$

For the DP, which satisfies $p_{\mathbf{A}} = p_{\mathbf{B}} = p$ and $P(F_{\mathbf{A}}^{\text{out}}) = P(F_{\mathbf{B}}^{\text{out}}) = P(F^{\text{out}})$, the above simultaneous Eqs. (5) and (6) come down to

$$P(F^{\text{out}}) = pP(F^{\text{out}})^3 + 1 - p, \#(7)$$

which has a solution for $1/3 \leq p \leq 1$ as follows.²⁸

$$P(F^{\text{out}}) = \left(\frac{1}{p} - \frac{3}{4}\right)^{\frac{1}{2}} - \frac{1}{2}. \#(8)$$

For the IM, which satisfies $p_{\mathbf{A}} = 1$, the above simultaneous Eqs. (5) and (6) come down to $P(F_{\mathbf{A}}^{\text{out}}) = P(F_{\mathbf{B}}^{\text{out}})^3$ and

$$P(F_{\mathbf{B}}^{\text{out}}) = p_{\mathbf{B}}P(F_{\mathbf{B}}^{\text{out}})^9 + 1 - p_{\mathbf{B}}. \#(9)$$

We can numerically calculate $P(F_{\mathbf{B}}^{\text{out}})$ (and $P(F_{\mathbf{A}}^{\text{out}})$) from Eq. (9).

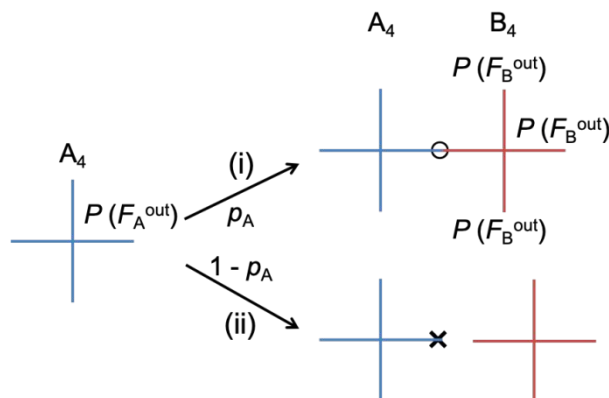


Fig. 3 How to calculate the probabilities that one arm of prepolymers (A_4) does not connect to the infinite-sized network ($P(F_{\mathbf{A}}^{\text{out}})$) in the mean-field approximation.

When a gel is formed, the simultaneous Eqs. (5) and (6) have a solution in the region of $0 \leq P(F_A^{\text{out}}) < 1$ and $0 \leq P(F_B^{\text{out}}) < 1$. Then, the conditions of gelation are²⁹

$$p \geq 1/3 \text{ (for the DP)} \quad (10)$$

$$p \geq 1/5 \text{ (for the IM)}. \quad (11)$$

Here, the critical connectivities for gelation (p_c) are significantly different, i.e., $p_c = 1/3$ for the DP and $p_c = 1/5$ for the IM.

Second, we explain how to calculate the number of the elastically effective chains (ν^{MF}) and the crosslinks (μ^{MF}) from the probability that A_4 or B_4 becomes a f -functional crosslink for $f=3$ and 4 ($P(X_{A3})$ or $P(X_{B3})$, respectively), which are described as

$$P(X_{A3}) = 4P(F_A^{\text{out}})[1 - P(F_A^{\text{out}})]^3 \#(12)$$

$$P(X_{B3}) = 4P(F_B^{\text{out}})[1 - P(F_B^{\text{out}})]^3 \#(13)$$

$$P(X_{A4}) = [1 - P(F_A^{\text{out}})]^4 \#(14)$$

$$P(X_{B4}) = [1 - P(F_B^{\text{out}})]^4 \#(15)$$

Since the tetra-functional prepolymers cannot play a role as a crosslink for $f=1$ and 2, the number per tetra-functional prepolymer of the elastically effective chains (ν^{MF}) and the crosslinks (μ^{MF}) are described as follows.

$$\nu^{\text{MF}} = s \left[\frac{3}{2}P(X_{A3}) + 2P(X_{A4}) \right] + (1-s) \left[\frac{3}{2}P(X_{B3}) + 2P(X_{B4}) \right] \#(16)$$

$$\mu^{\text{MF}} = s[P(X_{A3}) + P(X_{A4})] + (1-s)[P(X_{B3}) + P(X_{B4})]. \#(17)$$

Finally, by substituting $P(F_A^{\text{out}})$ and $P(F_B^{\text{out}})$ into Eqs. (16) and (17) with

$$\xi^{\text{MF}} = \nu^{\text{MF}} - \mu^{\text{MF}}, \#(18)$$

we obtain ξ^{MF} as a function of p as shown in Fig. 4. Here, the functions, which give ξ^{MF} for the DP and the IM, are denoted as $\xi_{\text{DP}}^{\text{MF}}(p)$ and $\xi_{\text{IM}}^{\text{MF}}(p)$, respectively. Whereas $\xi_{\text{DP}}^{\text{MF}}(p) = \xi_{\text{IM}}^{\text{MF}}(p)$ in the region of $p > 0.7$, $\xi_{\text{DP}}^{\text{MF}}(p) < \xi_{\text{IM}}^{\text{MF}}(p)$ in the region of $p < 0.7$, especially in the critical connectivity for gelation as shown in Eqs. (10) and (11). In other words, higher connectivity (i.e., $p_1 > p_2$) is needed in the DP to achieve $\xi_{\text{DP}}^{\text{MF}}(p_1) = \xi_{\text{IM}}^{\text{MF}}(p_2)$. The difference between the DP and the IM is stemmed from a correlation of connections. The connections in the DP distribute randomly. In contrast, the connections in the IM concentrate on the minor groups.

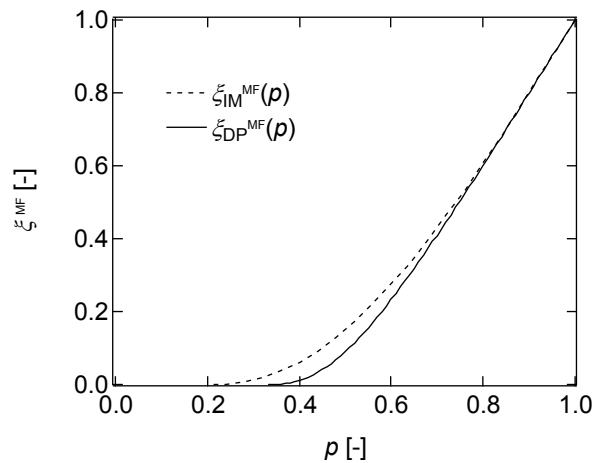


Fig. 4 $\xi^{\text{MF}} (\equiv \nu^{\text{MF}} - \mu^{\text{MF}})$ in the dynamic process (DP) and stoichiometrically imbalanced mixing (IM) as a function of the connectivity (p), predicted by mean-field approximation.

Materials and methods

a. Fabrication of Tetra-PEG gels

As a model prepolymer, we used tetra-maleimide-terminated poly(ethylene glycol) (Tetra-PEG-MA) and tetra-thiol-terminated poly(ethylene glycol) (Tetra-PEG-SH) which react mutually (Nippon Oil and Fat Co.). The terminal functionalization fractions of Tetra-PEG-MA (p_{MA}) and Tetra-PEG-SH (p_{SH}) were 95 and 93%, respectively, and the molecular weight of the prepolymers was 20 kg/mol. Constant amount of prepolymers (prepolymer concentration: 30, 60, and 120 g/L) were dissolved in phosphate-citrate buffer, where the ionic strength and the pH were 200 mM and 3.8, respectively. Here, the prepolymer concentration represents the ratio of the weight of the polymer to the solvent volume (not the solution volume). In the dynamic process (DP), the two prepolymer solutions were mixed in a stoichiometric ratio. On the other hand, in the stoichiometrically imbalanced mixing (IM), the two prepolymer solutions were mixed in different stoichiometrically imbalanced ratios, as shown in Table 1, so that we tune the connectivity after completion of the reaction.

b. Rheological measurement

In the DP, just after the mixing, the time courses of storage modulus (G_{DP}') and loss modulus (G_{DP}'') were measured at constant frequency (1 Hz), strain (1%), and temperature (25 °C) by rheometer (MCR301 and MCR302, Anton Paar, Austria), whereas in the IM, after completion of the reaction, storage modulus (G_{IM}') and loss modulus (G_{IM}'') were measured at the same conditions. In this paper, we regard the

storage modulus as elastic modulus on the basis of the extremely low energy dissipation of Tetra-PEG gel.³⁰

c. Ultraviolet-Visible light spectroscopy

To obtain the connectivity in the DP, we measured the time courses of the UV absorption at 310 nm were measured at constant temperature (25 °C) by Ultra-violet and visible spectrophotometric (JASCO V-630, Nihon-bunko, Japan). The cell thickness is 1 mm for 30 g/L and 5 mm for 60 and 120 g/L. According to our previous study,²⁶ the UV absorption peak of maleimide at 300nm overlapped with that of thioether bond at 250 nm. Thus, we measured at 310 nm to avoid the effect of the thioether bond.

Table 1. The sets of concentration of Tetra-PEG prepolymers (C) and weight mixing fraction of Tetra-PEG-MA to total prepolymers (s_w) for the IM.

C [g/L]	s_w [-]
30	0.5, 0.55, 0.6, 0.65, 0.7, 0.75
	0.25, 0.3, 0.35,
	0.4, 0.45, 0.5,
60	0.55, 0.6, 0.65,
	0.7, 0.75

120 0.5, 0.55, 0.6, 0.65, 0.7, 0.75

Results

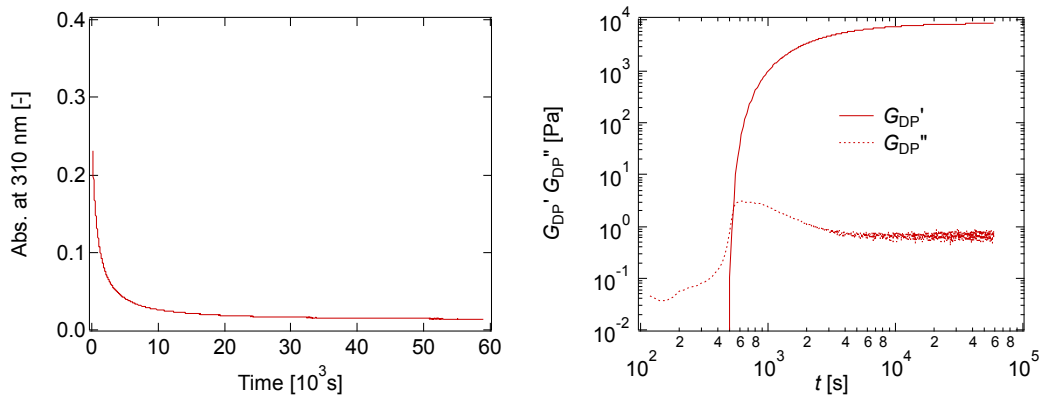
Due to their different molecular weights and functionalities, an equal weight of two prepolymers does not mean stoichiometric ratio. Therefore, we found the true stoichiometric ratio of two prepolymers (See Fig. 9 in Appendix). Based on the true stoichiometric ratio, we converted the weight mixing fraction of Tetra-PEG-MA to total prepolymers (s_w) to the molar mixing fraction (s).

In the dynamic process (DP), we mixed aqueous solutions of Tetra-PEG-MA and Tetra-PEG-SH in a stoichiometric ratio ($s = 0.5$) and measured the time courses of the UV absorption of maleimide at 310 nm and storage modulus (G_{DP}') and loss modulus (G_{DP}'') as an example shown in Fig. 5 (a) (All the data are given in Fig. 10 in Appendix). Because side reactions are negligible,²⁶ the connectivity (p) in the DP is estimated as

$$p = \left(1 - \frac{I_{310}(t)}{I_{310}(0)}\right)p_{MA,\#}(19)$$

where $I_{310}(t)$ and $p_{MA,\#}$ are the UV absorption at 310 nm after t seconds from the reaction initiation and the terminal functionalization fraction of Tetra-PEG-MA, respectively. By combining p - t and G_{DP}' - t relationships, we estimated elastic modulus (G_{DP})- p relationships for each prepolymer concentration (Fig. 6).

(a) The dynamic process (DP)



(b) The stoichiometrically imbalanced mixing (IM)

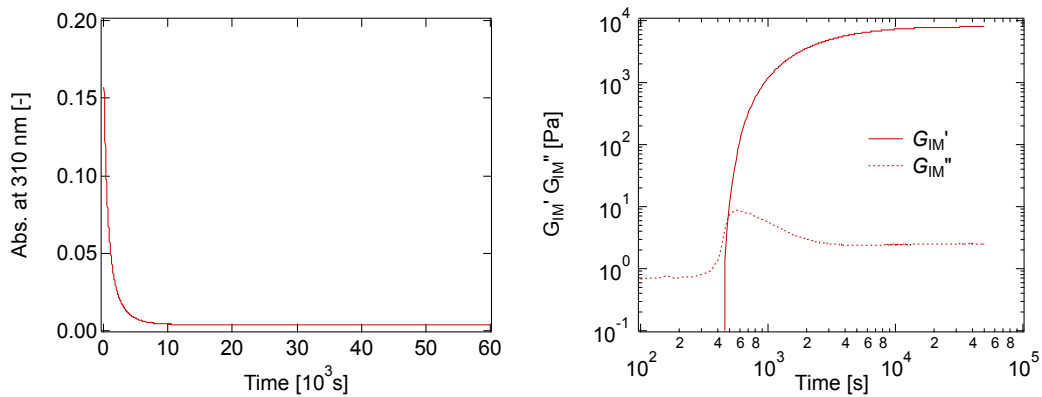


Fig. 5 (a) The time course of UV absorption at 310 nm per the optical path length of 1 mm and storage modulus (G_{DP}') and loss modulus (G_{DP}'') at 60 g/L in the dynamic process (DP). (b) The time course of UV absorption at 310 nm per the optical path length of 1 mm and G_{IM}' and G_{IM}'' at the weight mixing fraction of Tetra-PEG-MA to total prepolymers (s_w) = 0.45 at 60 g/L in the stoichiometrically imbalanced mixing (IM).

In the IM, we mixed an aqueous solution of the two prepolymers in a stoichiometrically imbalanced ratio ($s \neq 0.5$) and measured storage modulus (G_{IM}') and loss modulus (G_{IM}'') after completion of the reaction. We confirmed the completion of the reaction by observing that the values of the UV absorption at 310 nm and G_{IM}' reached equilibrium (Fig. 5 (b)). In the thiol excess gels, the equilibrium values of the UV absorptions were almost zero, which shows that the Tetra-PEG-MA reacted completely (Fig. 5 (b) left). Therefore, we assumed complete reaction of the minor group and estimated p in the IM as

$$p = \begin{cases} 2sp_{MA} & \left(\text{when } 0 \leq s \leq \frac{1}{2}\right) \\ 2(1-s)p_{SH} & \left(\text{when } \frac{1}{2} < s \leq 1\right). \end{cases} \quad \#(20)$$

where p_{SH} is the terminal functionalization fraction of Tetra-PEG-SH. Based on the combinations of G_{IM}' and p after completion of the reaction, we estimated $G_{IM}-p$ relationships for each prepolymer concentration (Fig. 6).

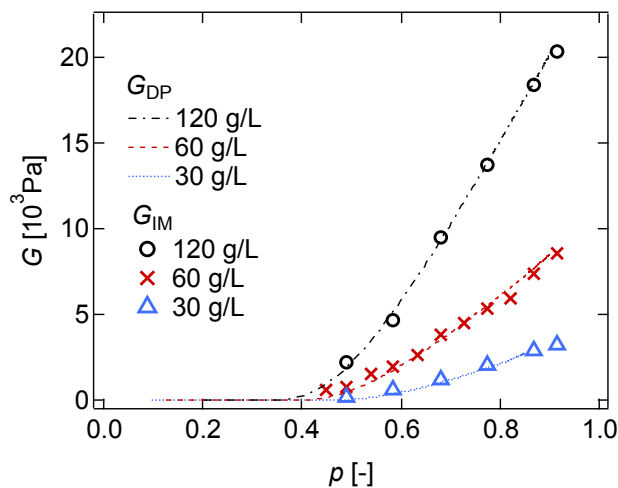


Fig. 6 Relationships between the elastic modulus (G) and the connectivity (p) in the dynamic process (DP) and the stoichiometrically imbalanced mixing (IM).

As shown in Fig. 6, in high p , G in the DP and the IM is almost the same; while in low p , G in the IM is slightly higher overall than in the DP. This tendency is the same as the theoretical prediction of Fig. 4, and the reason for this tendency would be also the same as the explanation of Fig. 4.

We then estimated the critical connectivity for gelation (p_c) in the DP and the IM. Although, in the mean-field approximation, p_c is defined as a minimum p showing the elasticity ($G > 0$) (Eqs. (7) and (8)), we determined the gelation threshold as the crossover point of G' and G'' ($G' = G''$) at the frequency of 1 Hz. Notably, according to Winter-Chambon's criterion,³¹ gelation point is defined as the point where the relationship $G' \sim G'' \sim \omega^\beta$. Although our criterion is different from that of Winter-Chambon, we have confirmed that both criteria, $G' = G''$ and $G' \sim G'' \sim \omega^\beta$, gives almost the same p_c . Table 2 shows p_c at different prepolymer concentrations (C). As C decreased, p_c in both the DP and the IM increased. At all C examined, p_c in the IM was less than p_c in the DP, qualitatively corresponding to the prediction by the mean-field approximation (MF). The C -dependence may be due to ineffective connections for network formation not considered in MF.

Table 2. The critical connectivity for gelation (p_c) in the dynamic process (DP) and the stoichiometrically imbalanced mixing (IM). The experimental results are shown on the first three lines and the theoretical prediction by the mean-field approximation (MF) is shown on the last line. We note that the theoretical prediction does not depend on the prepolymer concentrations (C).

C [g/L]	p_c in DP [-]	p_c in IM [-]
30	0.46	0.39
60	0.40	0.33
120	0.37	0.30
MF	0.33	0.20

Discussion

In the previous sections, in both the DP and the IM, (i) we theoretically calculated ξ^{MF} as a function of the connectivity (p) (Fig. 4), and (ii) experimentally determined elastic moduli (G_{DP} and G_{IM}) as a function of p (Fig. 6). In this section, by combining (i) and (ii), we show that the experimentally determined G_{DP} and G_{IM} are well described by the theoretically calculated $\xi_{\text{DP}}^{\text{MF}}(p)$ and $\xi_{\text{IM}}^{\text{MF}}(p)$, respectively, as

$$G_{\text{DP}} = g(C) \xi_{\text{DP}}^{\text{MF}}(p), \#(21)$$

$$G_{\text{IM}} = g(C) \xi_{\text{IM}}^{\text{MF}}(p). \#(22)$$

It is remarkable that the function $g(C)$ appearing in Eqs. (21) and (22) is common in both the DP and the IM and is independent of the connectivity p at high connectivity p (namely, g depends on the prepolymer concentration (C) and temperature).

Although we showed previously that Eq. (21) holds for the DP,²⁶ below we show that Eq. (22) holds even for the IM. In Fig. 7 (a), we plot the relationships between G_{IM} and $\xi_{\text{IM}}^{\text{MF}}(p)$ in the IM, where $\xi_{\text{IM}}^{\text{MF}}(p)$ is calculated with considering the terminal functionalization fractions of two prepolymers. Similar to the DP, G_{IM} is roughly proportional to $\xi_{\text{IM}}^{\text{MF}}(p)$, and downward deviation from the line is pronounced as p decreased. The deviation is most probably due to an increase in ineffective connections in low p ; that is, MF overestimates ξ_{IM} in low p . To extract the deviation from the linearity, we plot $G_{\text{IM}}/\xi_{\text{IM}}^{\text{MF}}$ ($= g$, according to Eq. (22)) as a function of p in Fig. 7 (b). The linearity holds in the region of $p > 0.7$ at $c = 60$ g/L or 120 g/L, while only holds in the region of $p > 0.8$ at 30 g/L. Notably, the overlapping concentration of the prepolymers (C^*) is about 40 g/L. Therefore, Eq. (22) is robust above C^* , while

become weaker below C^* ; that is, the effect of ineffective connections is likely to appear easily in lower C .

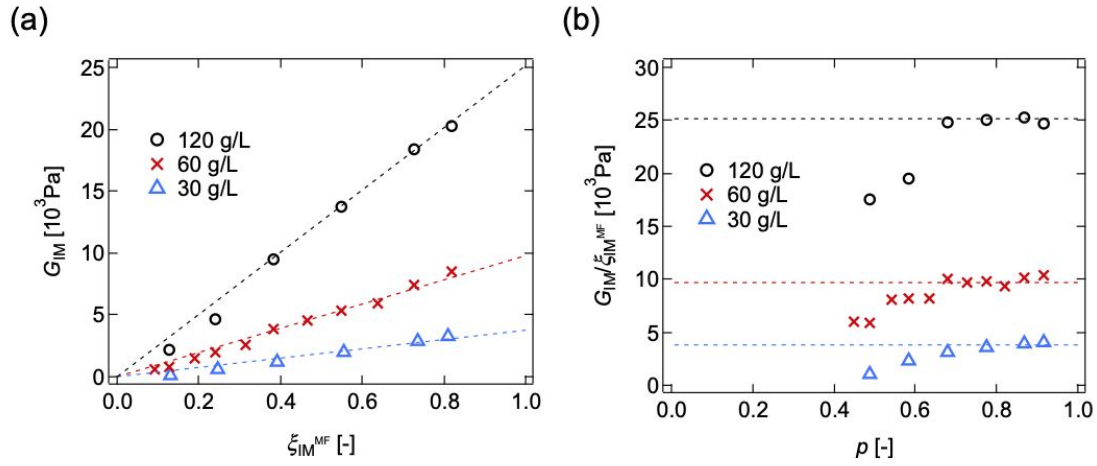


Fig. 7 (a) The relationships between G_{IM} and ξ_{IM}^{MF} . (b) G normalized by ξ_{IM}^{MF} as a function of p . The dashed lines show the approximate lines of data in high p .

In each of Eqs. (21) and (22), the right-hand side is theoretically calculated value (ξ^{MF}) shown in Fig. 4 and the left-hand side is experimentally measured value (G) shown in Fig. 6. In the following, we compare the DP and the IM by separating theoretical and experimental values.

First, we compare theoretically calculated $\xi_{DP}^{MF}(p)$ and $\xi_{IM}^{MF}(p)$. As shown in Fig. 4, the functions $\xi^{MF}=\xi_{DP}^{MF}(p)$ and $\xi^{MF}=\xi_{IM}^{MF}(p)$ have the different domains ($1/3 < p < 1$ and $1/5 < p < 1$, respectively) and the same ranges ($0 < \xi^{MF} < 1$). Thus, it is reasonable to compare the values of p in the same ξ^{MF} , rather than comparing the values of ξ^{MF} in

the same p . We plot the sets of p in the DP and the IM giving the same ξ^{MF} , i.e.,

$$\xi_{\text{DP}}^{\text{MF}}(p_1) = \xi_{\text{IM}}^{\text{MF}}(p_2), \text{ as the dashed line in Fig. 8.}$$

Second, we compare experimentally measured elastic moduli G_{DP} and G_{IM} . Considering Eqs. (21) and (22), it is natural to plot with $G_{\text{DP}}(p_1) = G_{\text{IM}}(p_2)$ as well as plotting with $\xi_{\text{DP}}^{\text{MF}}(p_1) = \xi_{\text{IM}}^{\text{MF}}(p_2)$. As shown in Fig. 8, the sets of p in the DP and the IM giving the same elastic moduli (the symbols) collapse onto a single master curve. Here, the symbols also include the sets of critical connectivity for gelation (p_c) in the DP and the IM from Table 2. Corresponding to Fig. 6, the symbols in Fig. 8 are roughly on the dotted line showing the equality of the DP and the IM in the region of $p > 0.7$. In contrast, in the region of $p < 0.7$, the deviation from the equality is pronounced. We note that the symbols are well reproduced by MF (dashed line in Fig. 8), although the deviation from the prediction of MF appears in low p in Fig. 7 (b). This suggests that in low p , MF overestimates ξ of the DP and the IM in the same way.

The consistency of MF prediction and the experiment with Tetra-PEG systems suggests that MF approximation could roughly predict gelation processes of the other polymer gels formed in various ways such as end-to-end reaction of prepolymers with different functional group numbers (A_xB_y) and radical polymerization.

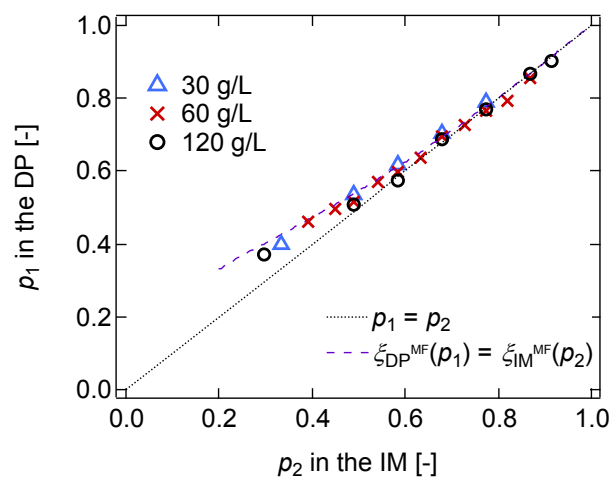


Fig. 8 Dashed line shows the relationship between connectivity (p_1) in the dynamic process (DP) and connectivity (p_2) in the stoichiometrically imbalanced mixing (IM) giving the same structural parameter, i.e., $\xi_{\text{DP}}^{\text{MF}}(p_1) = \xi_{\text{IM}}^{\text{MF}}(p_2)$. (See also Fig. 4 and its caption.) Symbols shows the sets of connectivity (p) in the DP and the IM giving the same elastic modulus (G) and the sets of critical connectivity for gelation (p_c) in the DP and the IM. Dotted line shows $p_1 = p_2$.

Conclusion

We compared the two methodologies tuning the connectivity in the gelation process of AB-type polymerization, i.e., the dynamic process (DP) and stoichiometrically imbalanced mixing (IM), by examining the effect of the connectivity on the elastic modulus of the Tetra-PEG gel. We obtained the following results: (i) the elastic modulus at the same connectivity in the DP and the IM was almost the same for each prepolymer concentration in high connectivity; and (ii) the critical connectivity for gelation of the IM was lower than that of the DP, which is stemmed from the distribution of the connections; that is, while the connections distribute randomly in the DP, the connections concentrate on the minor groups in the IM. We validated the mean-field approximation for the prediction of the connectivity dependence of the elastic modulus in sufficiently high prepolymer concentration and connectivity in the IM. The relationship between the DP and the IM was also well reproduced by the mean-field approximation in the wide region of prepolymer concentration and connectivity. These data will aid in elucidating the gelation process of polymer gels.

Appendix

1. Determination of the true stoichiometric weight ratio of two prepolymers

Before preparing a series of samples, we found the true stoichiometric weight ratio of prepolymers (s_{eq}); although two prepolymers were synthesized to have the same molecular weight and complete functionalization, they had different molecular weights and functionalities. We mixed Tetra-PEG-MA solutions (60 g/L) and Tetra-PEG-SH solutions with different concentrations (C_{SH}) and measured their UV absorptions at 310 nm after completion of the reaction (Fig. 9 (a)). The relationships between the absorptions and the concentrations of Tetra-PEG-SH (C_{SH}) were linear, reflecting high reaction conversion and negligible side reaction.²⁶ We estimated s_{eq} from the intercept of the line on the horizontal axis: $s_{eq} = 0.512$.

To further check the validity of this estimation, we mixed the prepolymer solutions in a stoichiometrically imbalanced prepolymer weight ratio, i.e., Tetra-PEG-MA : Tetra-PEG-SH = s_w : $1-s_w$, and measured the elastic modulus (G) after completion of the reaction at 60 g/L (Fig. 9 (b)). The G changed almost symmetrically against s_w with a peak around $s_w = 0.51$, corresponding to the UV estimation.

By accommodating s_{eq} and considering the terminal functionalization fractions of Tetra-PEG-MA and Tetra-PEG-SH ($p_{MA} = 0.95$ and $p_{SH} = 0.93$), molar mixing fraction (s) is described as

$$s = \frac{s_w(1 - s_{eq}) / p_{MA}}{s_w(1 - s_{eq}) / p_{MA} + (1 - s_w)s_{eq} / p_{SH}} \quad \#(1)$$

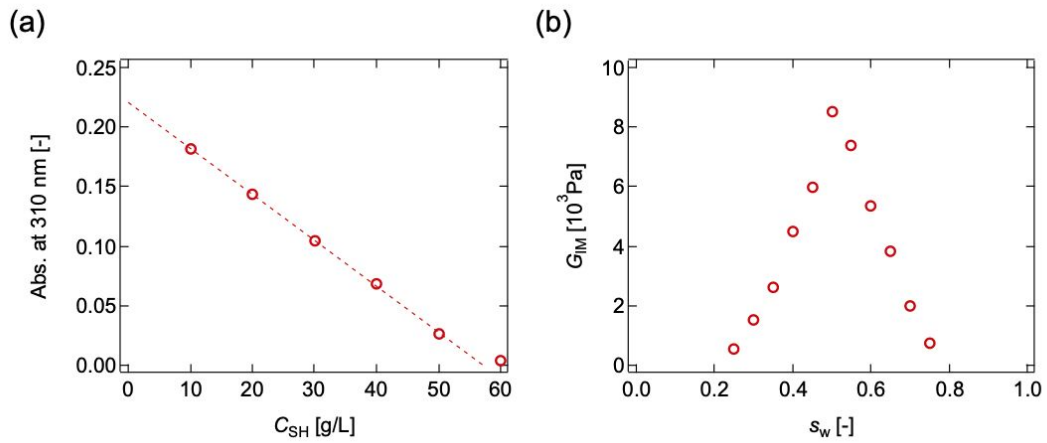
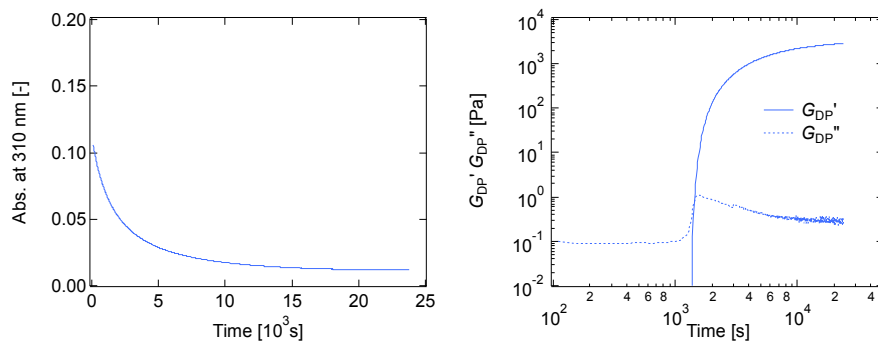


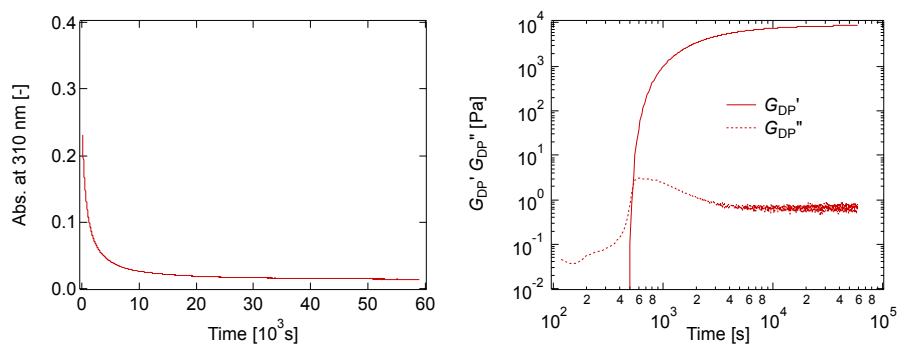
Fig 9. (a) The change of UV absorptions at 310 nm per the optical path length of 1 mm after completion of the gelation process with mixing Tetra-PEG-MA solutions (60 g/L) and Tetra-PEG-SH solutions (C_{SH}) (b) The change of the elastic modulus (G_{IM}) with mixing them in a stoichiometrically imbalanced prepolymer weight mixing fraction (Tetra-PEG-MA : Tetra-PEG-SH = s_w : $1-s_w$)

2. Spectroscopic and rheology measurements in the dynamic process (DP).

(a) 30 g/L



(b) 60 g/L



(c) 120 g/L

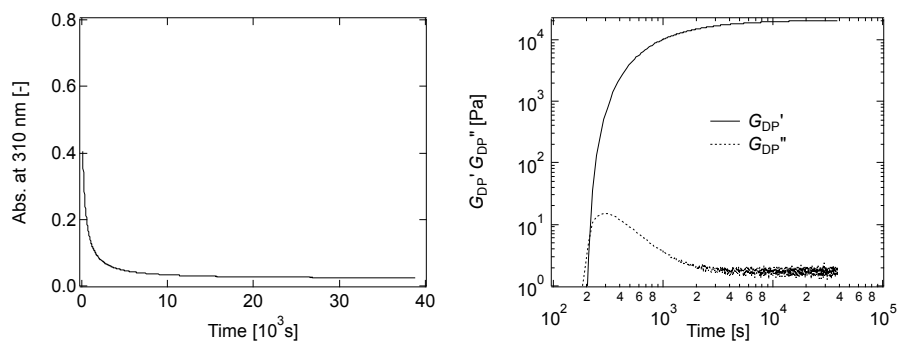


Fig. 10 The time course of UV absorption at 310 nm per the optical path length of 1 mm and storage modulus (G_{DP}') and loss modulus (G_{DP}'') at (a) 30 g/L, (b) 60 g/L, and (c) 120 g/L in the dynamic process (DP). (b) is the same as Fig. 5 (a).

Acknowledgement

This work was supported by the Japan Society for the Promotion of Science (JSPS) through the Grants-in-Aid for the Graduate Program for Leaders in Life Innovation (GPLLI), the International Core Research Center for Nanobio, Core-to-Core Program A. Advanced Research Networks, the Grants-in-Aid for Early Career Scientists Grant Number 19K14672, Scientific Research the Grants-in-Aid for Scientific Research (B) Grant Number 18H02027 to TS, and Scientific Research (S) Grant Number 16746899 to UC, and by Japan Science and Technology Agency (JST) through Center of Innovation (COI).

References

- 1 Y. Li, J. Rodrigues and H. Tomás, *Chem. Soc. Rev.*, 2012, **41**, 2193–2221.
- 2 B. Jeong, Y. H. Bae, D. S. Lee and S. W. Kim, *Nature*, 1997, **388**, 860–862.
- 3 A. Chenite, C. Chaput, D. Wang, C. Combes, M. D. Buschmann, C. D. Hoemann, J. C. Leroux, B. L. Atkinson, F. Binette and A. Selmani, *Biomaterials*, 2000, **21**, 2155–2161.
- 4 F. Chambon and H. H. Winter, *Polym. Bull.*, 1985, **13**, 499–503.
- 5 R. S. Whitney and W. Burchard, *Die Makromol. Chemie*, 1980, **181**, 869–890.
- 6 W. Burchard, K. Kajiwara, M. Gordon, J. Kálal, J. W. Kennedy and J. Kálal, *Macromolecules*, 1973, **6**, 642–649.
- 7 M. Gordon and K. Kajiwara, *Die Makromol. Chemie*, 1975, **176**, 2413–2435.

- 8 T. Sakai, T. Katashima, T. Matsushita and U. Chung, *Polym. J.*, 2016, **48**, 629–634.
- 9 F. Chambon and H. H. Winter, *J. Rheol. (N. Y. N. Y.)*, 1987, **31**, 683–697.
- 10 K. Urayama, T. Miki, T. Takigawa and S. Kohjiya, *Chem. Mater.*, 2004, **16**, 173–178.
- 11 S. M. G. Frankær, M. K. Jensen, A. G. Bejenariu and A. L. Skov, *Rheol. Acta*, 2012, **51**, 559–567.
- 12 S. Luňák and K. Dušek, *J. Polym. Sci. Polym. Symp.*, 1975, **53**, 45–55.
- 13 K. Dušek, M. Ilavský and S. Luňák, *J. Polym. Sci. Polym. Symp.*, 1975, **53**, 29–44.
- 14 K. Dušek and M. Ilavský, *J. Polym. Sci. Polym. Phys. Ed.*, 1983, **21**, 1323–1339.
- 15 M. Ilavský, L. M. Bogdanova and K. Dušek, *J. Polym. Sci. Polym. Phys. Ed.*, 1984, **22**, 265–278.
- 16 K. Dušek and M. Dušková-Smrčková, *Macromol. React. Eng.*, 2012, **6**, 426–445.
- 17 B. I. Voit and A. Lederer, *Chem. Rev.*, 2009, **109**, 5924–5973.
- 18 Y. Akagi, T. Katashima, Y. Katsumoto, K. Fujii, T. Matsunaga, U. Il Chung, M. Shibayama and T. Sakai, *Macromolecules*, 2011, **44**, 5817–5821.
- 19 Y. Akagi, J. P. Gong, U. Il Chung and T. Sakai, *Macromolecules*, 2013, **46**, 1035–1040.
- 20 T. Sakai, Y. Akagi, S. Kondo and U. Chung, *Soft Matter*, 2014, **10**, 6658–6665.
- 21 Y. Akagi, T. Katashima, H. Sakurai, U. Il Chung and T. Sakai, *RSC Adv.*, 2013, **3**, 13251–13258.

- 22 H. M. James and E. Guth, *J. Chem. Phys.*, 1953, **21**, 1039–1049.
- 23 C. W. Macosko and D. R. Miller, *Macromolecules*, 1976, **9**, 199–206.
- 24 D. R. Miller and C. W. Macosko, *Macromolecules*, 1976, **9**, 206–211.
- 25 M. Rubinstein and R. H. Colby, *Polymer Physics*, Oxford University Press, Oxford, 2003, Section 6.4.
- 26 K. Nishi, K. Fujii, U. Il Chung, M. Shibayama and T. Sakai, *Phys. Rev. Lett.*, 2017, **119**, 267801.
- 27 T. Sakai, T. Matsunaga, Y. Yamamoto, C. Ito, R. Yoshida, S. Suzuki, N. Sasaki, M. Shibayama and U. Il Chung, *Macromolecules*, 2008, **41**, 5379–5384.
- 28 Y. Akagi, T. Matsunaga, M. Shibayama, U. Il Chung and T. Sakai, *Macromolecules*, 2010, **43**, 488–493.
- 29 W. H. Stockmayer, *J. Polym. Sci.*, 1952, **9**, 69–71.
- 30 T. Sakai, Y. Akagi, T. Matsunaga, M. Kurakazu, U. Il Chung and M. Shibayama, *Macromol. Rapid Commun.*, 2010, **31**, 1954–1959.
- 31 H. H. Winter and F. Chambon, *J. Rheol. (N. Y. N. Y.)*, 1986, **30**, 367–382.